

## Supporting Information

### **ZIF-8/AuAg Nanocluster Composite as Fluorescent Sensor for Highly Sensitive and Selective Detection of Tetracycline**

Kexin Yan,<sup>a#</sup> Tianxia Chen,<sup>a#</sup> Siyi Li,<sup>a</sup> Peipei Cen,<sup>\*b</sup> Yan Guo<sup>a</sup> and Xiangyu Liu<sup>\*a</sup>

<sup>a</sup> State Key Laboratory of High-Efficiency Utilization of Coal and Green Chemical Engineering,  
College of Chemistry and Chemical Engineering, Ningxia University, Yinchuan 750021, China

<sup>b</sup> College of Public Health, Key Laboratory of Environmental Factors and Chronic Disease Control,  
Ningxia Medical University, Yinchuan 750004, China

# These authors contributed equally to this work.

\*Corresponding author

Prof. Xiangyu Liu

E-mail: xiangyuliu432@126.com

Dr. Peipei Cen

Email: 13895400691@163.com

## Contents:

### 1. Experimental Section

### 2. Supplementary Figures and Tables

Fig. S1 PXRD patterns of ZIF-8 and ZIF-8/AuAg NCs (a); FT-IR spectra of ZIF-8, AuAg NCs and ZIF-8/AuAg NCs (b).

Fig. S2 TEM image of AuAg NCs (a); TEM image of aggregated AuAg NCs (b).

Fig. S3 SEM images of: freshly prepared ZIF-8(a); ZIF-8/AuAg NCs (b).

Fig. S4 Content histogram of Au and Ag in the ZIF-8/AuAg nanocrystal composite.

Fig. S5 TGA of ZIF-8 and ZIF-8/AuAg NCs.

Fig. S6 Photographs of liquid AuAg NCs under UV light (a); Photographs of AuAg NCs after freezing (b).

Fig. S7 Fluorescence emission spectra of ZIF-8/AuAg NCs dispersion before and after the addition of TC, as well as those of the washed ZIF-8/AuAg NCs (a); A survey of the LOD for TC reported in the literature (b).

Fig. S8 FT-IR spectra of TC, ZIF-8/AuAg NCs and ZIF-8/AuAg NCs-TC (a); PXRD patterns of ZIF-8/AuAg NCs and ZIF-8/AuAg NCs-TC (b).

Table S1. The comparison of the LOD of different sensors for TC.

Table S2. Determinations of tetracycline in chicken and real water samples (n = 3).

Table S3. HOMO and LUMO energies calculated for DDTC and TC used at B3LYP/6-31G level.

### 3. References

# 1. Experimental

## 1. Reagents and instruments

All chemicals are reagent grade and commercially available. All chemicals are received for direct use without further purification. Transmission electron microscope (TEM) experiments are carried on a Hitachi HT7700 Transmission Electron Microscope. X-ray photoelectron spectroscopy (XPS) analyses are performed on an ESCALAB 250Xi system using Al K $\alpha$  X-ray. FT-IR spectra data are collected by an IR Affinity-21 Fourier Transform Infrared Spectrometer (4000-400 cm<sup>-1</sup>). The phase purity of the bulk or polycrystalline samples is measured by Powder X-ray diffraction (PXRD) measurements executed on a Rigaku RU200 diffractometer at 60 kV and 300 mA, using Cu K $\alpha$  radiation ( $\lambda = 1.5406 \text{ \AA}$ ), with a scan speed of 5° min<sup>-1</sup> and a step size of 0.02° in 2 $\theta$ . ultraviolet-visible absorption (UV-vis) spectra are collected on a Shimadzu UV-1800 UV-Visible Spectrophotometer. The fluorescence analyses are recorded with Hitachi F-7000 Fluorescence Spectrophotometer. Thermogravimetric analysis (TGA) is carried out on a STA8000 system analyzer under an N<sub>2</sub> atmosphere at a heating rate of 10 °C·min<sup>-1</sup> within the temperature ranging from 30 to 800 °C. Nitrogen adsorption/desorption isotherms are measured by a Tristar 2460 analyzer at the liquid nitrogen temperature. The samples are outgassed at 120 °C for 5 h before the measurements. The Brunauer Emmett Teller (BET) method is used to calculate the specific surface area from the adsorption data. Density functional theory (DFT) calculations are conducted by using the B3LYP/6-31G basis set implemented in the Gaussian 09 package.

## 1.2 Preparation of bimetallic AuAg NCs

A mixed solution was prepared by combining the HAuCl<sub>4</sub> solution (with a final concentration of 10 mM) and the AgNO<sub>3</sub> solution (with a final concentration of 10 mM), followed by the addition of diethyl dithiocarbamate (DDTC, 10 mM). Subsequently, an ascorbic acid solution (with a final concentration of 10 mM) was introduced into the above-mentioned mixed system. The resulting mixture was then subjected to heating in a 65 °C water bath for 1 h, ultimately leading to the formation

of a fluorescent gold-silver nanoclusters (AuAg NCs) solution.

### **1.3 Preparation of ZIF-8 framework**

ZIF-8 is synthesized in pure water system by improving the method reported in the literature. Add Zn (CH<sub>3</sub>HOO)<sub>2</sub> (10 mL, 0.3 g) solution dropwise to 2-methylimidazole (2-MIM, 10 mL, 1.12 g) aqueous solution and stir continuously (24 h). The resulting mixture was centrifuged three times at 3000 rpm (1157 g) to remove any unreacted solution. The obtained precipitate was dried in an oven at 45 °C, yielding a powdered form for subsequent use.

### **1.4 Preparation of AgAu NCs/ZIF-8 ratiometric fluorescent probe**

ZIF-8/AuAg NCs were synthesized by wet impregnation by adding AuAg NCs solution to the pre-synthesized ZIF-8 powder and ultrasonic treatment at room temperature for 70 min. The resulting slurry is dried to obtain the ZIF-8/AuAg NCs sample.

### **1.5 Sensing experiments of TC**

For the fluorescence quenching tests of TC, a typical experimental procedure was set up. TC powder samples were dissolved in deionized water, followed by ultrasonic treatment for 60 min to obtain a stable solution (0-22 μM). The fluorescence quenching behavior of the ZIF-8/AuAg NCs probe as a function of TC concentration was assessed by measuring the fluorescence intensity after immersion in different concentrations of TC solutions. Similarly, ZIF-8/AuAg NCs were immersed into various concentrations of TC solutions (0-28 μM), and the fluorescence intensities were recorded at an excitation wavelength of 365 nm. In order to verify the anti-interference ability of ZIF-8/AuAg NCs for TC fluorescence monitoring, different metal ions (Ni<sup>2+</sup>, Cr<sup>3+</sup>, Fe<sup>2+</sup>, Zn<sup>2+</sup>, Ba<sup>2+</sup>, Cd<sup>2+</sup>, Pb<sup>2+</sup>, Co<sup>2+</sup>, Cu<sup>2+</sup>, Mn<sup>2+</sup>, Ca<sup>2+</sup>, Ce<sup>4+</sup>) (2.0 μM) and organic molecules (penicillin, vitamin C, and urea) (2.0 μM) were tested, respectively. A TC solution (2.0 μM) was then added to the above solutions, and the fluorescence emission spectra of ZIF-8/AuAg NCs in these mixtures were measured again.

### **1.6 Experiment on fluorescence recovery performance after washing**

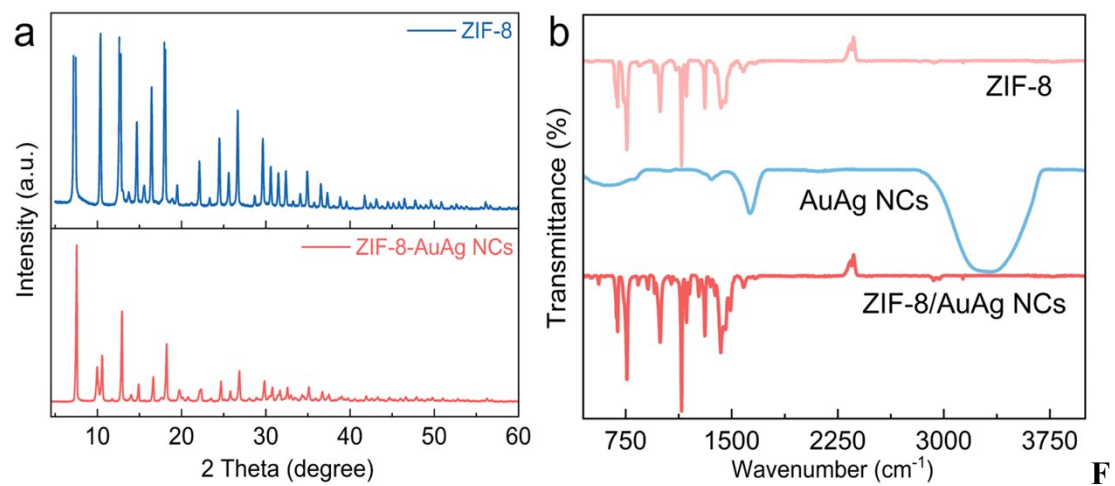
To evaluate the reusability of ZIF-8/AuAg NCs, their fluorescence recovery performance after washing with anhydrous ethanol was systematically investigated. After the fluorescence quenching detection with TC solutions, the ZIF-8/AuAg NCs

probe was collected by centrifugation and washed repeatedly with anhydrous ethanol to remove residual TC molecules adsorbed on the surface. The washed ZIF-8/AuAg NCs were redispersed in deionized water, and their fluorescence intensity was measured again under the same conditions (excitation wavelength of 365 nm).

### **1.7 Real sample analysis of chicken and water matrices**

Using ZIF-8/AuAg NCs to detect the TC residue levels in commercially available chicken and natural water environments known to be prone to TC contamination, the practicality of the ZIF-8/AuAg NCs-based sensor in TC residue detection in real environments is evaluated. A known concentration of TC solution was applied to the chicken samples and water samples, and then the samples are pretreated and processed into homogeneous solutions. Since there are many impurities in the processed samples, centrifugation was conducted to extract the supernatant for a purer sample. Subsequently, the supernatant samples of different concentrations were separately added to the ZIF-8/AuAg NCs solution. Changes in fluorescence intensity were recorded with a fluorescence spectrophotometer to obtain the corresponding concentrations, and the recovery rate is calculated.

## 2. Supplementary Figures and Tables.



**ig. S1** PXRD patterns of ZIF-8 and ZIF-8/AuAg NCs (a); FT-IR spectra of ZIF-8, AuAg NCs and ZIF-8/AuAg NCs (b).

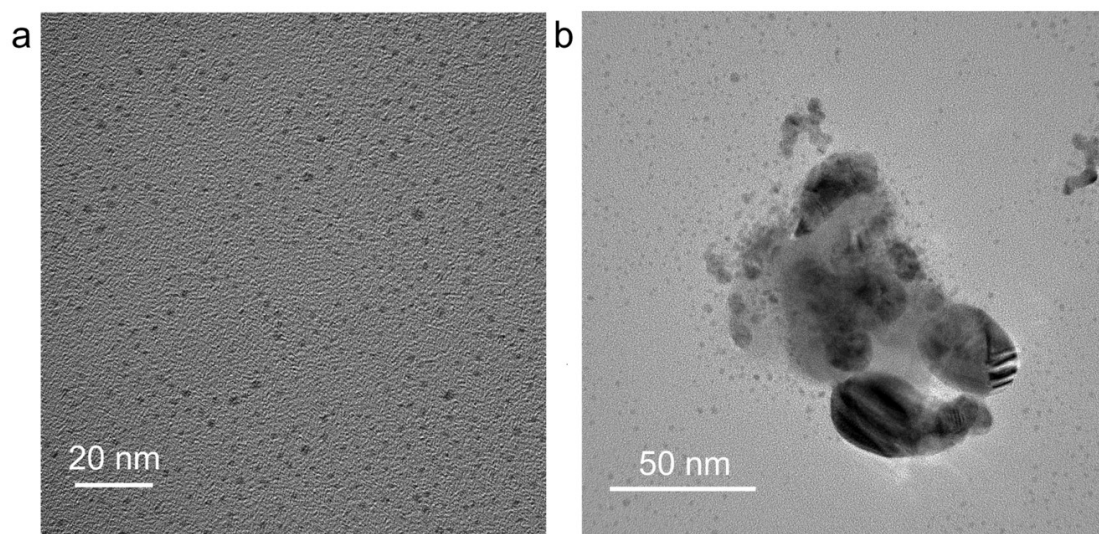


**Fig. S2** TEM image of AuAg NCs (a); TEM image of aggregated AuAg NCs (b).

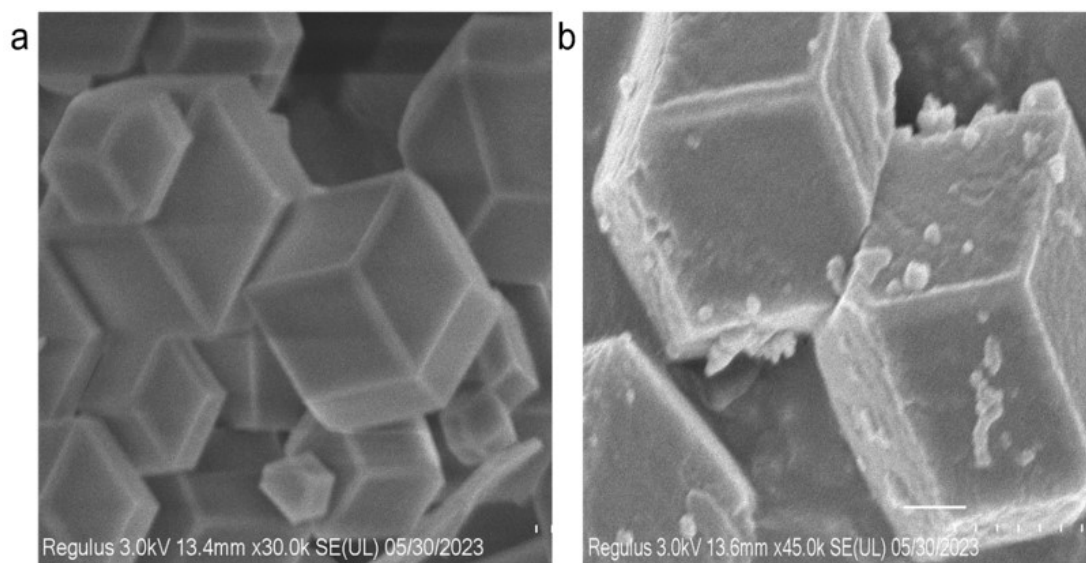


**Fig. S3** SEM images of: freshly prepared ZIF-8(a); ZIF-8/AuAg NCs (b).

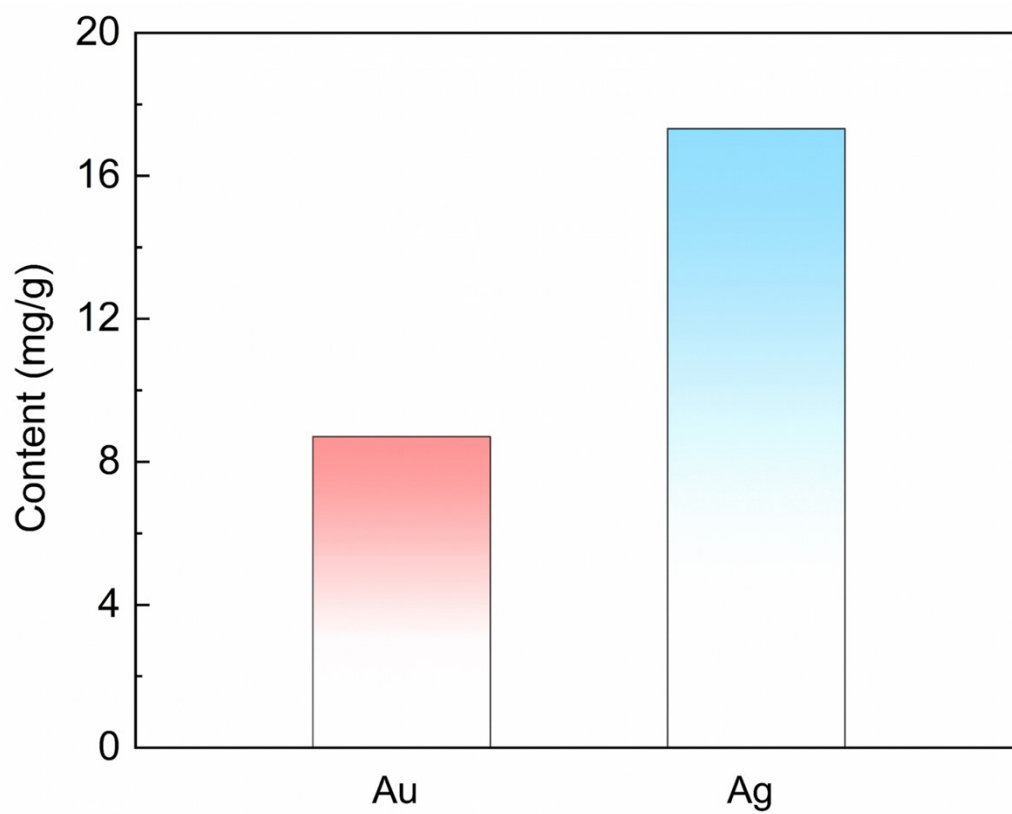


**Fig. S4** Content histogram of Au and Ag in the ZIF-8/AuAg nanocrystal composite.

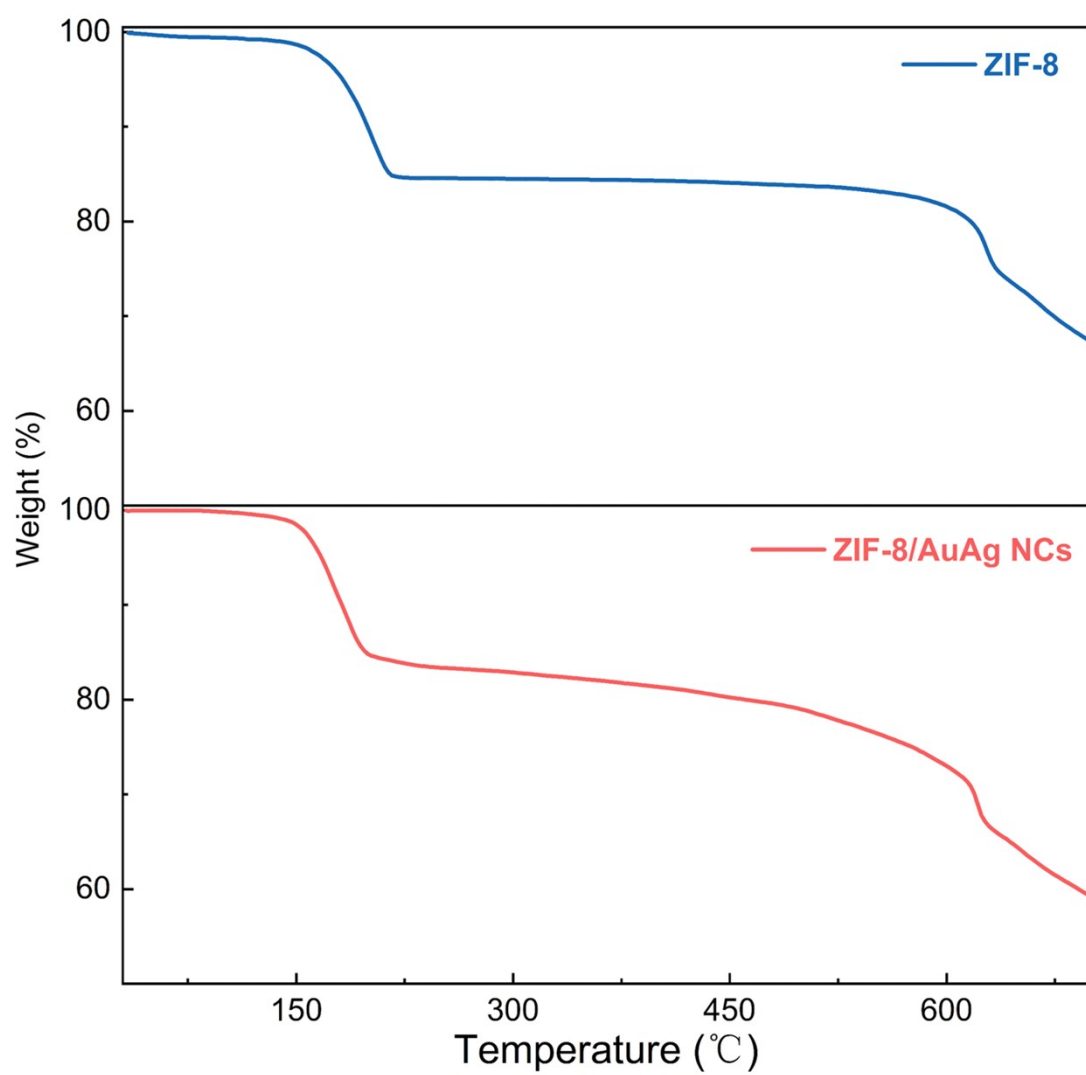


**Fig. S5** TGA of ZIF-8 and ZIF-8/AuAg NCs.

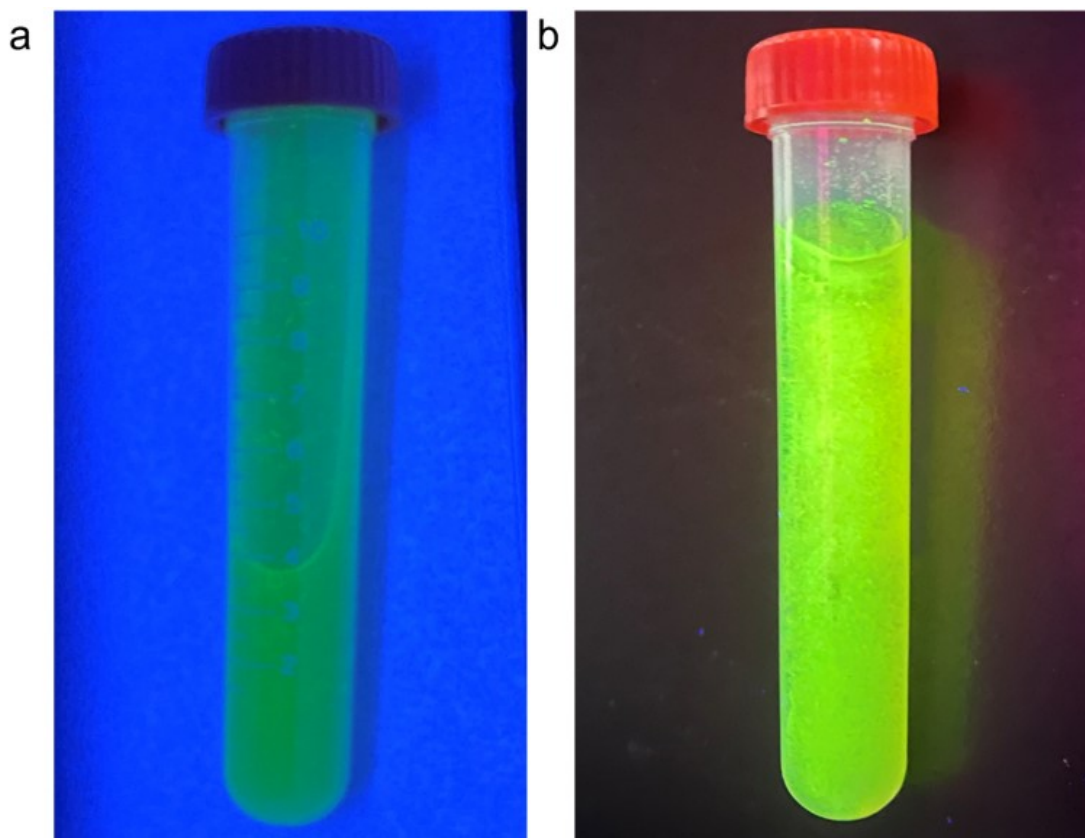


**Fig. S6** Photographs of liquid Au/Ag NCs under UV light (a); Photographs of Au/Ag NCs after freezing (b).

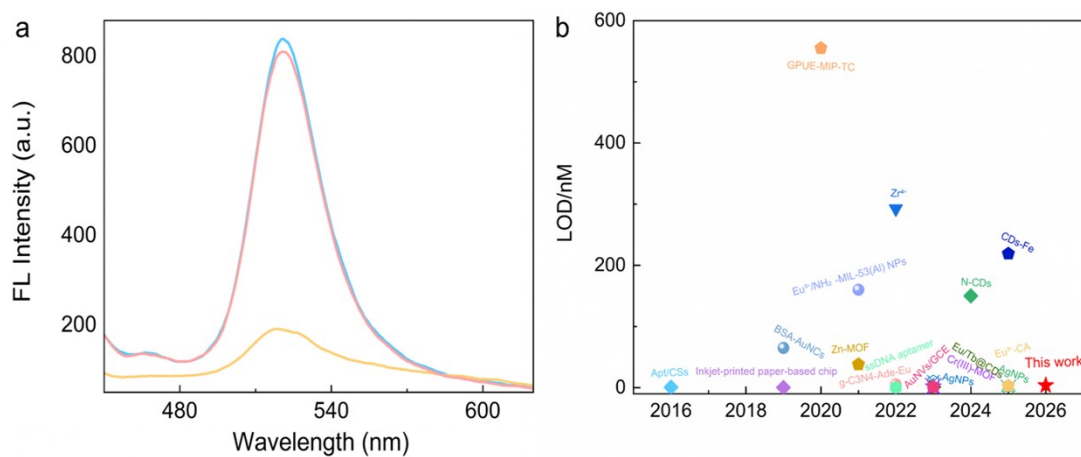


**Fig. S7** Fluorescence emission spectra of ZIF-8/AuAg NCs dispersion before and after the addition of TC, as well as those of the washed ZIF-8/AuAg NCs (a); A survey of the LOD for TC reported in the literature (b).

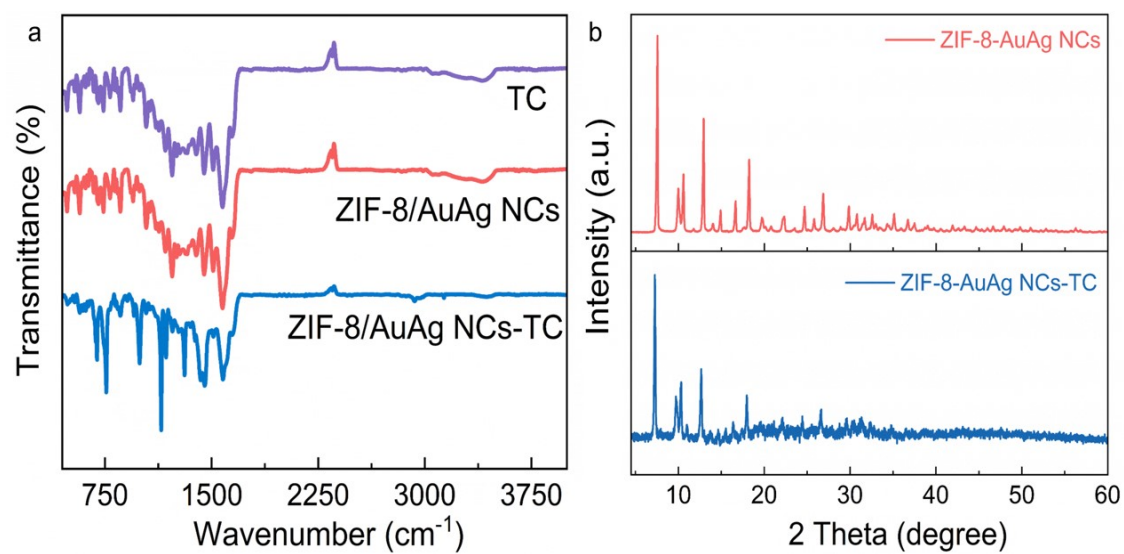


**Fig. S8** FT-IR spectra of TC, ZIF-8/AuAg NCs and ZIF-8/AuAg NCs-TC (a); PXRD patterns of ZIF-8/AuAg NCs and ZIF-8/AuAg NCs-TC (b).

**TableS1:** The comparison of the LOD of different sensors for TC.

Sensors	Date	LOD (nmol/ L)	Ref
g-C <sub>3</sub> NS <sub>64</sub> -Ade-Eu	2022	5	[1]
Ag NPs <sub>7</sub>	2023	10	[2]
Ag NPs	2025	0.16	[3]
Inkjet-printed paper-based chip	2019	0.11	[4]
Zn-MOF	2021	38	[5]
Eu/Tb@ CDs	2023	1	[6]
Ferrocene-labeled thiolated ssDNA aptamer	2022	0.16	[7]
Cr(III)-MOF	2023	1.76	[8]
Eu <sup>3+</sup> /NH <sub>2</sub> -MIL-53(Al) nanocomposites	2021	160	[9]
BSA-Au NCs	2019	65	[10]
Eu <sup>3+</sup> -CA	2025	3	[11]
Apt/CSs	2016	0.45	[12]
Au NVs/GCE	2023	1.19	[13]
Zr <sup>4+</sup>	2022	292.5	[14]
N-CDs	2024	150	[15]
GPUE-MIP-TC	2020	555	[16]
N, S-CDs	2025	219	[17]
<b>ZIF-8/AuAg NCs</b>	<b>2026</b>	<b>3.7</b>	<b>This work</b>

**Table S2:** Determinations of tetracycline in chicken and real water samples (n = 3)

Sample	Added ( $\mu\text{M}$ )	Mean found ( $\mu\text{M}$ )	Mean recovery (%)	RSD (%)
Chicken: 1	0.5	0.52	104	2.4
2	1	0.97	97	2.8
3	5	5.08	102	1.7
lake water: 1	0.5	0.48	96	3.1
2	1	1.02	102	2.1
3	5	4.87	97	1.6

---

Mean recovery (%) =  $100 \times (\text{c mean found} / \text{c added})$ .

---

**Table S3:** HOMO and LUMO energies calculated for APDC and TC used at B3LYP/6-31G level.

Compounds	LUMO (eV)	HOMO (eV)
DDTC	-0.96	-6.6
PDA	-0.81	-7.44

### 3. References

1. S. Zhang, Q. Sun, X. Liu, H. Li, J. Wang and M. Chen, *Sens. Actuators B-Chem.*, 2022, **372**, 132687.
2. S. Yang, C. Li, H. Zhan, R. Liu, W. Chen, X. Wang and K. Xu, *J. Nanobiotechnology.*, 2023, **21**, 22.
3. J. Xu, L. Wang, F. Hong, X. Lai, X. Wen and W. Yang, *J. Mater. Sci.*, 2026, **61**, 1053-1063.
4. J. Li, X. Wang, Y. Shan, H. Huang, D. Jian, L. Xue, S. Wang, and F. Liu, *Micromachines*, 2019, **10**, 27.
5. Chen, J., F. Xu, Q. Zhang, S. Li and X. Lu, *Analyst*, 2021, **146**, 6883-6892.
6. H. Che, Y. Nie, X. Tian and Y. Li, *J. Hazard. Mater.*, 2023, **441**, 129956.
7. K. Malecka-Baturo, A. Zaganiaris, I. Grabowska and K. Kurzątkowska-Adaszyńska, *Int. J. Mol. Sci.*, 2022, **23**, 13785.
8. A. Khezerlou, M. Tavassoli, M. Alizadeh Sani, Z. Ghasempour, A. Ehsani and B. Khalilzadeh *Food Chem. X*, 2023, **20**, 100883.
9. J. Chen, Y. Xu, S. Li, F. Xu and Q. Zhang, *RSC Adv.*, 2021, **11**, 2397-2404.
10. L. Meng, C. Lan, Z. Liu, N. Xu and Y. Wu, *Anal. Chim. Acta*, 2019, **1089**, 144
11. M. Jannatin, and Y. C. Chen, *Biosensors*, 2026, **16**, 29.
12. S. M. Taghdisi, N. M. Danesh, M. Ramezani and K. Abnous, *Biosens. Bioelectron.*, 2016, **85**, 509-514.
13. O. Hosu, G. Melinte, G. Ștefan, M. Casian and C. Cristea, *Electrochim. Acta*, 2023, **460**, 142556.
14. C. Saenjum, N. Pattapong, T. Aunsakol, T. Pattananandecha, S. Apichai, H. Murakami, K. Grudpan and N. Teshima, *J. Food Compos. Anal.*, 2022, **105**, 104215.
15. W. Yan, X. Wang, X. Gao and L. Zhao, *J. Photochem. Photobiol., A*, 2024, **447**, 115217.
16. J. E. S. Clarindo, R. B. Viana, P. Cervini, A. B. F. Silva and E. T. G. Cavalheiro, *Anal. Lett.*, 2020, **53**, 1932-1955.
17. M. Zhang, M. Zhang, S. Zhang, C. Tang and M. Hu, *Appl. Food Res.*, 2025, **5**, 101041.